



# Finite volume method for coupled subsurface flow problems, I: Darcy problem



Kirill M. Terekhov <sup>a,\*</sup>, Yuri V. Vassilevski <sup>a,b,c</sup>

<sup>a</sup> Marchuk Institute of Numerical Mathematics, Russian Academy of Sciences, Moscow, Russia

<sup>b</sup> Moscow Institute of Physics and Technology, Dolgoprudny, Russia

<sup>c</sup> Sechenov University, Moscow, Russia

## ARTICLE INFO

### Article history:

Received 14 July 2018

Received in revised form 30 April 2019

Accepted 5 June 2019

Available online 10 June 2019

### Keywords:

Darcy problem

Anisotropic diffusion

Finite-volume

Saddle-point

## ABSTRACT

The article introduces a finite-volume method for the Darcy problem in heterogeneous anisotropic media. The method is based on the mixed formulation for the pressure and its gradient. The method is stable despite collocation of both pressure and its gradient at cell centers and demonstrates the first order convergence on numerous benchmarks as well as good monotonicity property. The method produces quasi-definite matrix, which is numerically shown to have good asymptotics of the condition number. Our flux discretization method is a realization of our more general concept of stable flux discretization for saddle-point systems with vector of several unknowns. In this paper this vector is composed of pressure and its gradient and the saddle-point system is the mixed formulation of the Darcy problem.

© 2019 Elsevier Inc. All rights reserved.

## 1. Introduction

The cell-centered finite volume (FV) method is very popular due to conservation of the flux. However, the direct application of the method to saddle-point systems suffers from violation of Ladyzhenskaya-Babuška-Brezzi (LBB) condition [1]. We propose a FV method that is free of such instability for the diffusion problem generated by the Darcy law. Flows described by the Darcy law are fundamental in a number of subsurface engineering problems, such as petroleum reservoir engineering, environmental modeling, radionuclide migration. The subsurface media in the above applications is described by a heterogeneous permeability tensor. In terms of the basic Darcy problem this implies the anisotropic diffusion equation for which numerous FV methods have been proposed [2]. The mixed formulation of the Darcy problem with explicit degree of freedom for the velocity is very useful for reservoir simulators involving nonlinear extensions of Darcy law, such as Darcy-Forchheimer law and Brinkman form of Darcy law. In these cases the elimination of the velocity degrees of freedom is not feasible due to their nonlinear relation. For the sake of LBB-stability of the FV discretization of saddle-point coupled problems, the staggered degrees of freedom are usually applied [3,4]: the velocity degrees of freedom are staggered on cell faces and the pressure degrees of freedom are collocated at cell centers. Staggering complicates the use of general grids and satisfaction of conservation principles, although some progress have been made in this direction [5]. The alternative way to meet the LBB condition is a combination of the Rhie-Chow interpolation [6] and the collocation method which has become ubiquitous in most industrial applications. However, the implicit application of such interpolation results in large numerical stencils of the discretization.

\* Corresponding author.

E-mail addresses: [kirill.terekhov@gmail.com](mailto:kirill.terekhov@gmail.com) (K.M. Terekhov), [yuri.vassilevski@gmail.com](mailto:yuri.vassilevski@gmail.com) (Y.V. Vassilevski).

We consider the mixed formulation of the Darcy problem in terms of pressure and its gradient and obtain a saddle-point system of differential equations. We apply the FV method with collocated at cell centers pressure and gradient unknowns directly to the system and give a stable expression for the discrete flux. The flux discretization is linear and has the two-point stencil which is appealing in reservoir simulators. In addition, we suggest a general approach to incorporation of all boundary conditions (Dirichlet, Neumann, Robin) in the stable flux discretization. Another benefit of the method is that it avoids or at least minimizes spurious oscillations on non- $\mathbb{K}$ -orthogonal grids and retains the first order convergence, whereas the traditional linear two-point flux approximation FV method loses approximation properties [7]. We showed that there exists a solution of the produced linear system which has a quasi-definite matrix with good asymptotics of the condition number. We evaluate the method on a number of benchmarks and demonstrate the first order convergence and stability of the method.

The flux discretization technique suggested for the mixed formulation of the Darcy problem is a realization of our more general concept of stable flux discretization of saddle-point systems with vector of several unknowns (e.g. pressure and its gradient). The concept expresses a FV approximation of the vector flux on a cell face as a linear combination of collocated at neighboring cell centers unknown vectors with matrix coefficients. The latter matrices have non-negative eigenvalues and spectral radius less than one. For scalar unknowns this concept produces monotone FV methods. For vector unknowns this concept requires eigensplitting of the matrix which defines the discrete flux. The concept will be applied to other coupled problems of subsurface flow simulation such as the Biot equations and the incompressible elasticity equations. These problems will be addressed in subsequent papers. The idea of flux matrix eigensplitting is not new, it was suggested earlier for FV discretizations of Maxwell [8] and Navier-Stokes [9] equations on simple computational grids, in literature it is known as flux difference splitting and flux vector splitting [10], split upwinding [11].

This paper is organized as follows. In section 2 we give the mixed formulation of the Darcy problem and introduce the cell-centered FV method. In section 3 we address the stable flux discretization on interior mesh faces. In section 4 we discuss the stable flux discretization on boundary faces. In section 5 we give the numerical analysis of the scheme. In section 6 we present the numerical tests. The concluding remarks are collected afterwards.

## 2. Darcy problem and the finite volume method

We address the solution of the Darcy problem:

$$\begin{cases} -\nabla^T \mathbb{K} \nabla p = q & \text{in } \Omega, \\ \alpha p + \beta \mathbb{K} \nabla p \cdot \mathbf{n} = \gamma(\mathbf{x}) & \text{on } \partial\Omega, \end{cases} \quad (1)$$

where  $p \in H^1(\Omega)$  is the pressure satisfying the Dirichlet boundary conditions on a Dirichlet part of the domain boundary  $\partial\Omega$ . The polyhedral domain  $\Omega$  is covered by a polyhedral mesh  $\Omega_h$ ,  $\mathbb{K}$  is a given  $3 \times 3$  symmetric positive definite permeability tensor piecewise-constant on each polyhedral cell.

The first equation in (1) can be rewritten in the mixed formulation:

$$-\begin{bmatrix} \nabla & \\ \nabla^T \mathbb{K} & 0 \end{bmatrix} \begin{bmatrix} \mathbf{g} \\ p \end{bmatrix} = \begin{bmatrix} -\mathbf{g} \\ q \end{bmatrix}. \quad (2)$$

Here  $\mathbf{g}$  is the gradient of pressure. We note that  $\mathbf{g}$  is not the Darcy velocity  $\mathbf{u} = \mathbb{K} \nabla p$ , though the latter can be easily recovered from  $\mathbf{g}$ . Incorporation of the boundary condition is discussed in section 4.

Integrating (2) over a cell  $V \in \Omega_h$  and applying Gauss theorem we obtain:

$$\oint_{\partial V} \begin{bmatrix} \mathbf{n}^T \mathbb{K} & \mathbf{n} \\ \mathbf{n}^T \mathbb{K} & 0 \end{bmatrix} \begin{bmatrix} \mathbf{g} \\ p \end{bmatrix} dS = \int_V \begin{bmatrix} \mathbf{g} \\ -q \end{bmatrix} dV. \quad (3)$$

We rewrite (3) in the equivalent formulation:

$$\sum_{f \in \mathcal{F}(V)} \begin{bmatrix} \mathbf{n}_f^T \mathbb{K} & \mathbf{n}_f \\ \mathbf{n}_f^T \mathbb{K} & 0 \end{bmatrix} \begin{bmatrix} \mathbf{g}_f \\ p_f \end{bmatrix} |f| = \sum_{f \in \mathcal{F}(V)} \mathbf{F} |f| = \begin{bmatrix} \mathbf{g}_V \\ -q_V \end{bmatrix} |V|, \quad (4)$$

where  $\mathcal{F}(V)$  is the set of faces of the cell  $V$ ,  $|f|$  and  $|V|$  are area of the face  $f$  and volume of the cell  $V$ , respectively,  $p_f$  and  $\mathbf{g}_f$  are averaged pressure and its gradient on face  $f$ ,  $\mathbf{g}_V$  and  $q_V$  are averaged gradient and the source term on cell  $V$ .

The key question in the finite volume method is how to calculate the flux  $\mathbf{F}$  on face  $f$ . From (4) the flux  $\mathbf{F}$  is defined by matrix  $A$ :

$$\mathbf{F} = A \begin{bmatrix} \mathbf{g}_f \\ p_f \end{bmatrix}, \quad A = \begin{bmatrix} \mathbf{n}_f^T \mathbb{K} & \mathbf{n}_f \\ \mathbf{n}_f^T \mathbb{K} & 0 \end{bmatrix}. \quad (5)$$

The flux definition (5) involves matrix  $A$  whose negative eigenvalue may cause instability. To cope with this, we split matrix  $A$  into a sum of singular matrices

$$A = A^+ + A^-, \tag{6}$$

where  $A^+$  has one positive eigenvalue and  $A^-$  has one negative eigenvalue,

$$A^\pm = \frac{1}{2} \begin{bmatrix} \pm m^{-1} \mathbf{n}_f \mathbf{n}_f^T \mathbb{K} & \mathbf{n}_f \\ \mathbf{n}_f^T \mathbb{K} & \pm m \end{bmatrix} = N^\pm \begin{bmatrix} \mathbb{K} \\ 1 \end{bmatrix}, \tag{7}$$

with

$$N^\pm \equiv \frac{1}{2} \begin{bmatrix} \pm m^{-1} \mathbf{n}_f \mathbf{n}_f^T & \mathbf{n}_f \\ \mathbf{n}_f^T & \pm m \end{bmatrix} = \frac{1}{2} \begin{bmatrix} \pm m^{-1} \mathbf{n}_f \\ 1 \end{bmatrix} \begin{bmatrix} \mathbf{n}_f^T & \pm m \end{bmatrix}. \tag{8}$$

In principle, any choice of positive  $m$  is possible, however, consideration of impermeable material suggests  $\mathbb{K}$ -dependence of  $m$ . Splitting (6) is used for stabilization of otherwise unstable flux defined by (5).

### 3. Flux discretization on interior faces

Let  $f$  be an interior face shared by cells  $V_1$  and  $V_2$ ,  $f = V_1 \cap V_2$ . The normal  $\mathbf{n}_f$  of face  $f$  is directed from  $V_1$  towards  $V_2$ . The idea behind the stabilization of the discrete flux is to use the matrix coefficient with a negative eigenvalue for the values collocated at cell  $V_1$  and the matrix coefficient with a positive eigenvalue for the values collocated at cell  $V_2$ . Let  $\mathbb{K}_1$  and  $\mathbb{K}_2$  be the permeability tensors at  $V_1$  and  $V_2$ , respectively. Let matrix coefficients  $A_1 = A_1^+ + A_1^-$  and  $A_2 = A_2^+ + A_2^-$  be splittings (6)-(7) defined by  $\mathbb{K}_1$  and  $\mathbb{K}_2$ , respectively. Let also  $\mathbf{g}_{f,1}$  and  $\mathbf{g}_{f,2}$  be the gradients of pressure on interface  $f$  from the side of  $V_1$  and  $V_2$ , respectively. We write one-sided first-order discretizations of flux (5) on  $f$ :

$$\mathbf{F} = A_1^- \left( \begin{bmatrix} \mathbf{g}_1 \\ p_1 \end{bmatrix} + O(h) \right) + A_1^+ \begin{bmatrix} \mathbf{g}_{f,1} \\ p_f \end{bmatrix} = A_2^+ \left( \begin{bmatrix} \mathbf{g}_2 \\ p_2 \end{bmatrix} + O(h) \right) + A_2^- \begin{bmatrix} \mathbf{g}_{f,2} \\ p_f \end{bmatrix}. \tag{9}$$

Due to (2) the Darcy velocity belongs to the space  $H(\text{div}, \Omega)$  and so its normal component is continuous,  $\mathbf{n}_f^T \mathbf{u}_f = \mathbf{n}_f^T \mathbb{K}_1 \mathbf{g}_{f,1} = \mathbf{n}_f^T \mathbb{K}_2 \mathbf{g}_{f,2}$ , whereas due to factorization of  $N^\pm$  in (8) only normal component of  $\mathbf{u}_f$  is required in (9). Therefore, the face degrees of freedom  $\mathbf{n}_f^T \mathbf{u}_f$  and  $p_f$  can be eliminated from the continuity equation (9) and the flux discretization becomes:

$$\mathbf{F} = N_1^+ (N_1^+ - N_2^-)^\dagger A_2^+ \begin{bmatrix} \mathbf{g}_2 \\ p_2 \end{bmatrix} - N_2^- (N_1^+ - N_2^-)^\dagger A_1^- \begin{bmatrix} \mathbf{g}_1 \\ p_1 \end{bmatrix} + O(h), \tag{10}$$

where pseudo-inverse matrix  $(N_1^+ - N_2^-)^\dagger$  is

$$(N_1^+ - N_2^-)^\dagger = \left( \frac{m_1 + m_2}{2} \begin{bmatrix} (m_1 m_2)^{-1} \mathbf{n}_f \mathbf{n}_f^T & \mathbf{0} \\ \mathbf{0}^T & 1 \end{bmatrix} \right)^\dagger = \frac{2}{m_1 + m_2} \begin{bmatrix} m_1 m_2 \mathbf{n}_f \mathbf{n}_f^T & \mathbf{0} \\ \mathbf{0}^T & 1 \end{bmatrix}, \tag{11}$$

for any positive  $m_1$  and  $m_2$ .

Plugging (11) into (10) gives:

$$\mathbf{F} = \frac{1}{m_1 + m_2} \left( \begin{bmatrix} \mathbf{n}_f \mathbf{n}_f^T \mathbb{K}_2 & m_2 \mathbf{n}_f \\ m_1 \mathbf{n}_f^T \mathbb{K}_2 & m_1 m_2 \end{bmatrix} \begin{bmatrix} \mathbf{g}_2 \\ p_2 \end{bmatrix} + \begin{bmatrix} -\mathbf{n}_f \mathbf{n}_f^T \mathbb{K}_1 & m_1 \mathbf{n}_f \\ m_2 \mathbf{n}_f^T \mathbb{K}_1 & -m_1 m_2 \end{bmatrix} \begin{bmatrix} \mathbf{g}_1 \\ p_1 \end{bmatrix} \right) + O(h). \tag{12}$$

Note that in (12) we obtain the matrix coefficient for the degrees of freedom collocated at cells  $V_i$  with one non-zero eigenvalue  $(-1)^i (\mathbf{n}_f^T \mathbb{K}_i \mathbf{n}_f + m_1 m_2) / (m_1 + m_2)$ . Formula (12) defines the discrete flux on interior faces  $f$  contributing to (4).

### 4. Flux discretization on boundary faces

Let  $f$  be a boundary face belonging to cell  $V_1$  with permeability  $\mathbb{K}_1$ . The center of  $f$  is denoted by  $\mathbf{x}_f$ , the normal  $\mathbf{n}_f$  is oriented outwards of  $V_1$ . The flux on the boundary is approximated with the first order of accuracy by:

$$\mathbf{F} = \tilde{A}^+ \begin{bmatrix} \mathbf{g}_f \\ p_f \end{bmatrix} + \tilde{A}^- \left( \begin{bmatrix} \mathbf{g}_1 \\ p_1 \end{bmatrix} + O(h) \right). \tag{13}$$

The singular matrices  $\tilde{A}^+$  and  $\tilde{A}^-$  are chosen so that  $A = \tilde{A}^+ + \tilde{A}^-$  and the use of face degrees of freedom  $\mathbf{g}_f$  and  $p_f$  may be replaced by the boundary condition in (1)

$$\begin{bmatrix} \beta \mathbf{n}_f^T \mathbb{K}_1 & \alpha \end{bmatrix} \begin{bmatrix} \mathbf{g}_f \\ p_f \end{bmatrix} = \gamma_f, \tag{14}$$

where  $\gamma_f = \frac{1}{|f|} \int_f \gamma(\mathbf{x}) dS$ .

We consider two non-symmetric splittings of  $A$ . The first splitting is based on matrices  $\tilde{A}_D^+$  and  $\tilde{A}_D^-$  for Dirichlet type boundary conditions:

$$\tilde{A}_D^+ = \begin{bmatrix} \mathbf{0}^T & \mathbf{n}_f \\ \mathbf{n}_f^T \mathbb{K}_1 & -m_1 \end{bmatrix}, \quad \tilde{A}_D^- = \begin{bmatrix} \mathbf{n}_f^T \mathbb{K}_1 & -m_1 \end{bmatrix}. \tag{15}$$

Splitting (15) does not require the values of  $\mathbf{g}_f$  to calculate (13). The second splitting is based on matrices  $\tilde{A}_N^+$  and  $\tilde{A}_N^-$  for Neumann type boundary conditions:

$$\tilde{A}_N^+ = \begin{bmatrix} m_1^{-1} \mathbf{n}_f \mathbf{n}_f^T \mathbb{K}_1 & \mathbf{0} \\ \mathbf{n}_f^T \mathbb{K}_1 & 0 \end{bmatrix}, \quad \tilde{A}_N^- = \begin{bmatrix} -m_1^{-1} \mathbf{n}_f \mathbf{n}_f^T \mathbb{K}_1 & \mathbf{n}_f \\ 0 & 0 \end{bmatrix}. \tag{16}$$

Splitting (16) does not require the value of  $p_f$  to calculate (13).

Finally, we define

$$\tilde{A}^\pm = \mu_D \tilde{A}_D^\pm + \mu_N \tilde{A}_N^\pm, \quad \mu_D = \frac{\alpha}{\alpha + \beta m_1}, \quad \mu_N = \frac{\beta m_1}{\alpha + \beta m_1}. \tag{17}$$

Factorization of matrices  $\tilde{A}_D^+$  and  $\tilde{A}_N^+$

$$\tilde{A}_D^+ = \begin{bmatrix} \mathbf{n}_f \\ m_1 \end{bmatrix} \begin{bmatrix} \mathbf{0}^T & 1 \end{bmatrix}, \quad \tilde{A}_N^+ = m_1^{-1} \begin{bmatrix} \mathbf{n}_f \\ m_1 \end{bmatrix} \begin{bmatrix} \mathbf{n}_f^T \mathbb{K}_1 & 0 \end{bmatrix} \tag{18}$$

results in the simple definition of  $\tilde{A}^+$ :

$$\tilde{A}^+ = \frac{1}{\alpha + \beta m_1} \begin{bmatrix} \mathbf{n}_f \\ m_1 \end{bmatrix} \begin{bmatrix} \beta \mathbf{n}_f^T \mathbb{K}_1 & \alpha \end{bmatrix}. \tag{19}$$

Note that (19) requires only the boundary condition (14) to calculate (13). The final expression for flux (13) is:

$$\mathbf{F} = \frac{1}{\alpha + \beta m_1} \left( \begin{bmatrix} \mathbf{n}_f \\ m_1 \end{bmatrix} \gamma_f + \begin{bmatrix} -\beta \mathbf{n}_f \mathbf{n}_f^T \mathbb{K}_1 & \beta m_1 \mathbf{n}_f \\ \alpha \mathbf{n}_f^T \mathbb{K}_1 & -\alpha m_1 \end{bmatrix} \begin{bmatrix} \mathbf{g}_1 \\ p_1 \end{bmatrix} \right) + O(h). \tag{20}$$

Formula (20) defines the discrete flux needed to calculate (4) on boundary face  $f$ . Definition (20) provides the first-order approximation. The matrix  $\tilde{A}^-$  has one non-zero eigenvalue  $\lambda = \frac{\beta + \alpha m_1}{\alpha + \beta m_1}$ . In our numerical experiments we use

$m_i = (\mathbf{n}_f^T \mathbb{K}_i \mathbf{n}_f)^{3/2}$  for interior and boundary faces. This choice of  $m_i$  minimizes overshoots and undershoots of the numerical solution. We chose the parameter  $m_i$  basing on trial and error: according to our experience, small parameters  $m_i$  destroy solution monotonicity, whereas large parameters  $m_i$  deteriorate convergence rate to zero.

### 5. Numerical analysis

The numerical analysis is done under the following assumptions:

**Assumption 1.** The mesh  $\Omega_h$  is simply-connected.

**Assumption 2.** The permeability tensor  $\mathbb{K}$  is symmetric positive-definite on all the cells of the mesh  $\Omega_h$ .

Let  $|\mathcal{V}(\Omega_h)|$  denote the number of mesh cells and global vectors  $\mathbf{g} \in \mathfrak{R}^{3|\mathcal{V}(\Omega_h)|}$  and  $p \in \mathfrak{R}^{|\mathcal{V}(\Omega_h)|}$  represent gradients and pressures at mesh cells. Let matrices  $I_{\mathbf{g}_1} \in \mathfrak{R}^{3|\mathcal{V}(\Omega_h)| \times 3}$  and  $I_{p_1} \in \mathfrak{R}^{|\mathcal{V}(\Omega_h)| \times 1}$  denote the elementary assembling matrices for local gradient  $\mathbf{g}_1$  and pressure  $p_1$  unknowns, i.e.  $I_{\mathbf{g}_1}$  has one unity in each column and zeros in the other entries and  $I_{p_1}$  has the only unity so that

$$I_{\mathbf{g}_1}^T \mathbf{g} = \mathbf{g}_1, \quad I_{p_1}^T p = p_1, \tag{21}$$

for global gradient  $\mathbf{g}$  and global pressure  $p$  vectors. For each pair of neighboring cells we define face assembling matrices  $I_{\mathbf{g}_{1,2}} \in \mathfrak{R}^{3|\mathcal{V}(\Omega_h)| \times 6}$  and  $I_{p_{1,2}} \in \mathfrak{R}^{|\mathcal{V}(\Omega_h)| \times 2}$ :

$$I_{\mathbf{g}_{1,2}} = [ I_{\mathbf{g}_1} \quad I_{\mathbf{g}_2} ], \quad I_{p_{1,2}} = [ I_{p_1} \quad I_{p_2} ]. \tag{22}$$

During the assembling of the linear system, the contribution of fluxes on internal faces (12), boundary faces (20) and right hand side to the system matrix  $J$  is represented by blocks:

$$\begin{aligned}
 J \begin{bmatrix} \mathbf{g} \\ p \end{bmatrix} &= \sum_{f \in \mathcal{F}(\Omega_h \setminus \partial\Omega_h)} \frac{|f|}{m_1 + m_2} \begin{bmatrix} I_{\mathbf{g}_{1,2}} & \\ & I_{p_{1,2}} \end{bmatrix} \begin{bmatrix} \mathbf{n}_f \mathbf{n}_f^T \mathbb{K}_1 & -\mathbf{n}_f \mathbf{n}_f^T \mathbb{K}_2 & -m_1 \mathbf{n}_f & -m_2 \mathbf{n}_f \\ -\mathbf{n}_f \mathbf{n}_f^T \mathbb{K}_1 & \mathbf{n}_f \mathbf{n}_f^T \mathbb{K}_2 & m_1 \mathbf{n}_f & m_2 \mathbf{n}_f \\ -m_2 \mathbf{n}_f^T \mathbb{K}_1 & -m_1 \mathbf{n}_f^T \mathbb{K}_2 & m_1 m_2 & -m_1 m_2 \\ m_2 \mathbf{n}_f^T \mathbb{K}_1 & m_1 \mathbf{n}_f^T \mathbb{K}_2 & -m_1 m_2 & m_1 m_2 \end{bmatrix} \begin{bmatrix} \mathbf{g}_1 \\ \mathbf{g}_2 \\ p_1 \\ p_2 \end{bmatrix} \\
 &+ \sum_{f \in \mathcal{F}(\partial\Omega_h)} \frac{|f|}{\alpha + \beta m_1} \begin{bmatrix} I_{\mathbf{g}_1} & \\ & I_{p_1} \end{bmatrix} \begin{bmatrix} \beta \mathbf{n}_f \mathbf{n}_f^T \mathbb{K}_1 & -\beta m_1 \mathbf{n}_f \\ -\alpha \mathbf{n}_f^T \mathbb{K}_1 & \alpha m_1 \end{bmatrix} \begin{bmatrix} \mathbf{g}_1 \\ p_1 \end{bmatrix} \\
 &+ \sum_{V_1 \in \mathcal{V}(\Omega_h)} |V_1| \begin{bmatrix} I_{\mathbf{g}_1} & \\ & I_{p_1} \end{bmatrix} \begin{bmatrix} \mathbf{g}_1 \\ 0 \end{bmatrix},
 \end{aligned} \tag{23}$$

where  $\mathcal{F}(\Omega_h \setminus \partial\Omega_h)$ ,  $\mathcal{F}(\partial\Omega_h)$  and  $\mathcal{V}(\Omega_h)$  are the set of internal faces, boundary faces and cells, respectively.

The assembling results in a matrix with  $2 \times 2$  block form that can be factorized:

$$J \begin{bmatrix} \mathbf{g} \\ p \end{bmatrix} = \begin{bmatrix} AK + V & B_1 \\ B_2^T K & C \end{bmatrix} \begin{bmatrix} \mathbf{g} \\ p \end{bmatrix} = \begin{bmatrix} A + VK^{-1} & B_1 \\ B_2^T & C \end{bmatrix} \begin{bmatrix} K & \\ & I \end{bmatrix} \begin{bmatrix} \mathbf{g} \\ p \end{bmatrix} = J_{\mathbf{u}} \begin{bmatrix} K\mathbf{g} \\ p \end{bmatrix}, \tag{24}$$

here  $K = \text{diag}(\mathbb{K}_1, \mathbb{K}_2, \dots, \mathbb{K}_n)$  is the block-diagonal matrix of permeabilities,  $V = \text{diag}(|V_1|\mathbb{I}, |V_2|\mathbb{I}, \dots, |V_n|\mathbb{I})$  is the block-diagonal matrix of cell volumes. Matrix  $J_{\mathbf{u}}$  corresponds to the formulation with Darcy velocity  $K\mathbf{g}$ . Under Assumptions 1 and 2, matrix  $A$  is generalized symmetric block irreducible Z-matrix with positive-definite diagonal blocks, negative semi-definite off-diagonal blocks, zero block row-sum for internal cells and positive semi-definite block row-sum on cells next to the boundary with non-zero  $\beta$ , matrix  $C$  is symmetric irreducible M-matrix with zero row-sum for internal cells and positive row-sum on cells next to the boundary with non-zero  $\alpha$ . According to [12], matrix  $C$  is positive semi-definite in general and is definite if  $\alpha$  is nonzero on a part of  $\partial\Omega_h$ . According to [13], matrix  $A$  is a generalized M-matrix, that does not imply the invertibility of  $A$ .

**Lemma 1.** Matrix  $A + VK^{-1}$  is positive definite.

**Proof.**  $VK^{-1}$  is positive definite under Assumption 2. Matrix  $A$  is assembled from positive semi-definite factors of rank 1:

$$AK\mathbf{g} = \sum_{f \in \mathcal{F}(\Omega \setminus \partial\Omega)} \frac{|f|}{m_1 + m_2} I_{\mathbf{g}_{1,2}} \begin{bmatrix} \mathbf{n}_f \\ -\mathbf{n}_f \end{bmatrix} \begin{bmatrix} \mathbf{n}_f^T & -\mathbf{n}_f^T \end{bmatrix} \begin{bmatrix} \mathbb{K}_1 \mathbf{g}_1 \\ \mathbb{K}_2 \mathbf{g}_2 \end{bmatrix} + \sum_{f \in \mathcal{F}(\partial\Omega)} \frac{\beta |f|}{\alpha + \beta m_1} I_{\mathbf{g}_1} \mathbf{n}_f \mathbf{n}_f^T \begin{bmatrix} \mathbb{K}_1 \mathbf{g}_1 \end{bmatrix}. \tag{25}$$

Therefore, matrix  $A + VK^{-1}$  is positive definite.  $\square$

**Lemma 2.** Matrix  $J_{\mathbf{u}}$  is weakly quasi-definite.

**Proof.** Matrix  $A + VK^{-1}$  is positive definite. Matrix  $C$  is positive semi-definite and may have a kernel associated with a constant vector. If we show that  $B_1 = -B_2$ , then matrix  $J_{\mathbf{u}}$  is symmetric provided we flip the sign for equations associated with pressure and hence it is weakly quasi-definite. The assembling of  $B_1$  and  $B_2^T$  matrices gives:

$$\begin{aligned}
 B_1 p &= \sum_{f \in \mathcal{F}(\Omega_h \setminus \partial\Omega_h)} \frac{|f|}{m_1 + m_2} I_{\mathbf{g}_{1,2}} [\mathbb{I}_{2 \times 2} \otimes \mathbf{n}_f] \begin{bmatrix} -m_1 & -m_2 \\ m_1 & m_2 \end{bmatrix} \begin{bmatrix} p_1 \\ p_2 \end{bmatrix} + \sum_{f \in \mathcal{F}(\partial\Omega_h)} \frac{-\beta m_1 |f|}{\alpha + \beta m_1} I_{\mathbf{g}_1} \mathbf{n}_f p_1, \\
 B_2^T K\mathbf{g} &= \sum_{f \in \mathcal{F}(\Omega_h)} \frac{|f|}{m_1 + m_2} I_{p_{1,2}} \begin{bmatrix} -m_2 & -m_1 \\ m_2 & m_1 \end{bmatrix} [\mathbb{I}_{2 \times 2} \otimes \mathbf{n}_f^T] \begin{bmatrix} \mathbb{K}_1 \mathbf{g}_1 \\ \mathbb{K}_2 \mathbf{g}_2 \end{bmatrix} + \sum_{f \in \mathcal{F}(\partial\Omega_h)} \frac{-\alpha |f|}{\alpha + \beta m_1} I_{p_1} \mathbf{n}_f^T \mathbb{K}_1 \mathbf{g}_1 \\
 &= \sum_{f \in \mathcal{F}(\Omega_h \setminus \partial\Omega_h)} I_{p_{1,2}} \left( |f| \begin{bmatrix} -1 & \\ & 1 \end{bmatrix} - \frac{|f|}{m_1 + m_2} \begin{bmatrix} -m_1 & -m_2 \\ m_1 & m_2 \end{bmatrix} \right) [\mathbb{I}_{2 \times 2} \otimes \mathbf{n}_f^T] \begin{bmatrix} \mathbb{K}_1 \mathbf{g}_1 \\ \mathbb{K}_2 \mathbf{g}_2 \end{bmatrix} \\
 &+ \sum_{f \in \mathcal{F}(\partial\Omega_h)} I_{p_1} \left( |f| \begin{bmatrix} -1 \\ \end{bmatrix} + \frac{\beta m_1 |f|}{\alpha + \beta m_1} \right) \mathbf{n}_f^T \mathbb{K}_1 \mathbf{g}_1 \\
 &= - \sum_{V_1 \in \mathcal{V}(\Omega_h)} I_{p_1} \left( \sum_{f \in \mathcal{F}(V_1)} |f| \mathbf{n}_f^T \right) \mathbb{K}_1 \mathbf{g}_1 - B_1^T K\mathbf{g} = -B_1^T K\mathbf{g},
 \end{aligned} \tag{26}$$

since  $\sum_{f \in \mathcal{F}(V_1)} |f| \mathbf{n}_f^T = \mathbf{0}^T$ , where  $\mathcal{F}(V_1)$  denotes the set of faces for cell  $V_1$  and normal  $\mathbf{n}_f$  is directed outwards of  $V_1$ .

Formula (26) implies  $B_1 = -B_2$  and weak quasi-definiteness of  $J_{\mathbf{u}}$ .  $\square$

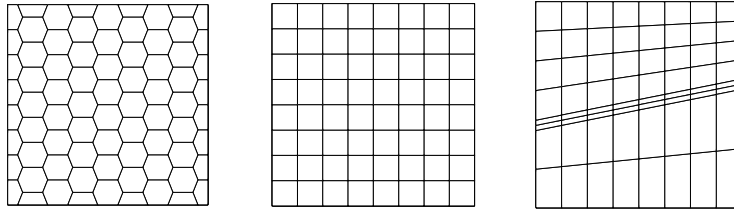


Fig. 1. Grids for benchmarks with known analytic solution: hexagonal (left), square (middle), oblique barrier (right).

**Theorem 3.** The solution to the FV problem (4), (12), (20) exists.

**Proof.** When Dirichlet boundary condition is present on a part of  $\partial\Omega_h$ , at least one row-sum of matrix  $C$  is positive and the matrix is positive-definite, thus the inverse of  $J_u$  is quasi-definite according to [14] and the solution to the system (4), (12), (20) exists. When only Neumann boundary condition is set, then matrix  $C$  is semi-definite and according to [14,15] a non-unique solution exists due to the fact that pseudo-inverse of  $J_u$  is a weakly quasi-definite matrix.  $\square$

## 6. Numerical experiments

### 6.1. Problems with known analytic solutions

We consider 2D benchmark problems with known analytic solutions: mild anisotropy, strong anisotropy and oblique barrier (tests 1.1, 5 and 7 in [16]), non-symmetric tensor (test 3 in [17]), discontinuous tensor modified for 2D (test 4 from [18]), locking problem with Neumann boundary condition, anisotropy parameter  $\epsilon = 10^{-5}$  and constraint on zero pressure integral (definition close to [19]). The computational domain is  $\Omega = [0, 1]^2$ , its boundary  $\partial\Omega$  is of Dirichlet type for all the problems except the locking problem. We measure  $L_2$ -norms of errors in discrete pressure  $p_h$  and Darcy velocity  $\mathbf{u}_h = \mathbb{K}\mathbf{g}_h$ . The FV solutions are calculated on grids presented schematically in Fig. 1. The grids for the oblique barrier problem and the problem with discontinuous tensor are aligned with tensor discontinuities. All these benchmarks are challenging and are used to test the robustness of discretization methods.

The accuracy of the numerical solution is presented in Table 1. The convergence rate demonstrated by the method for the Darcy velocity on average is 0.8. Note that the choice  $m_i = 1$  provides  $O(h)$  convergence with possible violations of the discrete maximum principle. Thus we prefer to use  $m_i = (\mathbf{n}_f^T \mathbb{K}_i \mathbf{n}_f)^{3/2}$ . For the locking problem on hexagonal grid, the convergence is almost lost for the pressure, in other cases the numerical pressure demonstrates close to the first order convergence. In all the problems except for the locking problem, the boundary conditions are of Dirichlet type. The locking problem is non-singular due to additional constraint on pressure integral. We estimate the condition number of  $J$ ,  $\text{cond}(J)$ , as the ratio of the spectral radii of  $J$  and  $J^{-1}$ . Table 1 demonstrates  $O(h^{-1})$  asymptotics of  $\text{cond}(J)$ .

### 6.2. Problems with wells

First, we test the method on two problems which are used to assess monotonicity of the method. The first problem has two wells separated by a small number of cells and homogeneous Neumann boundary condition on the outer boundary. The second problem has a well in the middle of the domain and homogeneous Dirichlet boundary condition on the outer boundary. In both problems the permeability tensor  $\mathbb{K}$  is strongly anisotropic, with rotated axes of anisotropy, the wells are represented by square holes with given Dirichlet boundary conditions (0 and 1 on each of two wells, 1 on the single well) [20]. According to the maximum principle, in both problems the differential solution belongs to  $[0, 1]$ . Our numerical solution of the first problem remains in the interval  $[0.0316, 0.968]$  on the coarse  $11 \times 11$  grid and  $[0.000696, 0.9993]$  on the fine  $88 \times 88$  grid. The condition numbers are  $\text{cond}(J) = 575289$  on  $11 \times 11$  grid and  $\text{cond}(J) = 4.697 \times 10^6$  on  $88 \times 88$  grid, that indicates to  $O(h^{-1})$  asymptotics (see Fig. 2).

The numerical solution of the second problem has a tiny undershoot: it belongs to  $[-0.00018 : 0.809]$  on  $9 \times 9$  grid,  $[-8.64 \times 10^{-5} : 0.976]$  on  $54 \times 54$  grid and  $[-1.31 \times 10^{-6} : 0.995]$  on  $216 \times 216$  grid (each grid is generated by a random perturbation of a square grid). The condition number exhibits  $O(h^{-1})$  asymptotics as well:  $\text{cond}(J) = 481120$  on  $9 \times 9$  grid,  $\text{cond}(J) = 2.884 \times 10^6$  on  $54 \times 54$  grid,  $\text{cond}(J) = 1.154 \times 10^7$  on  $216 \times 216$  grid. Tiny violation of the discrete maximum principle (DMP) is not surprising: to the best of our knowledge and [21], no consistent linear FV method with a compact stencil can provide the DMP for a general Darcy problem (see Fig. 3).

Second, we consider a grid with non-flat faces and a heterogeneous permeability field from the realistic Norne field provided by the open porous media initiative data [22]. In order to apply properly the method, we have to ensure that the divergence is zero for a constant function on each cell of the mesh. To this end, we triangulated non-flat mesh faces and applied (4) for general polyhedral cells. We setup three wells with prescribed bottom hole pressure which define the right hand side in (4)  $q_V = WI(p_{V_i, bhp} - p_{V_i})$ . We place the wells at the cells located at  $\mathbf{x}_{V_1} = (4.567 \times 10^5, 7.321 \times 10^6, 2.768 \times 10^3)$ ,

**Table 1**  
Error norms and condition numbers of  $J$  for the problems with analytic solution.

Problem \ $h^{-1}$		8	16	32	64	128	256
Mild anisotropy rectangular	$\ p_h - p\ _{L_2}$	0.43	0.223	0.114	0.0584	0.0296	0.0149
	order	–	0.95	0.961	0.971	0.981	0.988
	$\ \mathbf{u}_h - \mathbf{u}\ _{L_2}$	2.25	1.428	0.84	0.472	0.259	0.14
	order	–	0.657	0.765	0.83	0.867	0.889
	cond( $J$ )	58.8	117.6	234.8	469.9	939.9	1879.4
Mild anisotropy hexagonal	$\ p_h - p\ _{L_2}$	0.412	0.217	0.112	0.0568	0.0287	0.0144
	order	–	0.924	0.959	0.976	0.986	0.992
	$\ \mathbf{u}_h - \mathbf{u}\ _{L_2}$	2.04	1.286	0.769	0.447	0.256	0.146
	order	–	0.667	0.743	0.782	0.801	0.809
	cond( $J$ )	68.6	120	215.1	397.4	759.4	1481.1
Strong anisotropy rectangular	$\ p_h - p\ _{L_2}$	0.788	0.463	0.276	0.16	0.091	0.05
	order	–	0.767	0.749	0.784	0.821	0.853
	$\ \mathbf{u}_h - \mathbf{u}\ _{L_2}$	0.202	0.12	0.074	0.048	0.0314	0.0209
	order	–	0.753	0.69	0.63	0.606	0.59
	cond( $J$ )	116.2	315.4	692.7	1419.9	2856.8	5718.5
Strong anisotropy hexagonal	$\ p_h - p\ _{L_2}$	0.85	0.531	0.314	0.177	0.097	0.052
	order	–	0.681	0.757	0.824	0.872	0.907
	$\ \mathbf{u}_h - \mathbf{u}\ _{L_2}$	0.223	0.145	0.102	0.0725	0.0502	0.0337
	order	–	0.622	0.512	0.486	0.53	0.576
	cond( $J$ )	174.6	422.9	1006	2059.1	3925.1	7160.2
Non-symmetric tensor rectangular	$\ p_h - p\ _{L_2}$	0.0267	0.0198	0.013	0.0078	0.00436	0.00234
	order	–	0.434	0.603	0.742	0.838	0.899
	$\ \mathbf{u}_h - \mathbf{u}\ _{L_2}$	0.577	0.4	0.252	0.149	0.0844	0.0467
	order	–	0.528	0.665	0.76	0.819	0.853
	cond( $J$ )	32	63.99	130.5	268.5	551.8	1115.3
Non-symmetric tensor hexagonal	$\ p_h - p\ _{L_2}$	0.02	0.0146	0.00926	0.0535	0.00291	0.00153
	order	–	0.471	0.656	0.791	0.876	0.928
	$\ \mathbf{u}_h - \mathbf{u}\ _{L_2}$	0.464	0.32	0.202	0.122	0.0714	0.0414
	order	–	0.536	0.662	0.734	0.769	0.784
	cond( $J$ )	33.7	59	107.1	204.6	404.8	815
Locking rectangular	$\ p_h - p\ _{L_2}$	546.2	273.1	136.6	68.3	34.14	17.07
	order	–	1	1	1	1	1
	$\ \mathbf{u}_h - \mathbf{u}\ _{L_2}$	0.000818	0.000421	0.000214	0.000107	$5.37 \times 10^{-5}$	$2.67 \times 10^{-5}$
	order	–	0.958	0.979	0.992	1	1.007
	cond( $J$ )	$1.01 \times 10^{10}$	$1.01 \times 10^{10}$	$1.02 \times 10^{10}$	$1.04 \times 10^{10}$	$1.08 \times 10^{10}$	$1.16 \times 10^{10}$
Locking hexagonal	$\ p_h - p\ _{L_2}$	0.7	0.697	0.694	0.688	0.677	0.657
	order	–	0.00613	0.00664	0.0123	0.0235	0.0435
	$\ \mathbf{u}_h - \mathbf{u}\ _{L_2}$	0.00231	0.00122	0.000665	0.000377	0.000222	0.000139
	order	–	0.923	0.873	0.821	0.762	0.681
	cond( $J$ )	43061.2	154369	582511	$2.26 \times 10^6$	$8.9 \times 10^6$	$3.52 \times 10^7$
Oblique barrier	$\ p_h - p\ _{L_2}$	0.00878	0.00486	0.00258	0.00134	0.000685	0.000347
	order	–	0.854	0.912	0.946	0.968	0.982
	$\ \mathbf{u}_h - \mathbf{u}\ _{L_2}$	0.0607	0.03	0.0149	0.00743	0.00371	0.00186
	order	–	1.016	1.012	1.004	1.0001	0.999
	cond( $J$ )	4379.9	7502.8	8581.3	8774.3	13141.1	26326.7
Discontinuous tensor rectangular	$\ p_h - p\ _{L_2}$	0.166	0.091	0.0484	0.0252	0.0129	0.00652
	order	–	0.866	0.91	0.944	0.967	0.981
	$\ \mathbf{u}_h - \mathbf{u}\ _{L_2}$	2.335	1.326	0.724	0.387	0.204	0.107
	order	–	0.816	0.872	0.905	0.923	0.934
	cond( $J$ )	373.4	734.4	1451.7	2882.9	5734.4	11463.8

$\mathbf{x}_{V_2} = (4.609 \times 10^5, 7.323 \times 10^6, 2.598 \times 10^3)$  and  $\mathbf{x}_{V_3} = (4.595 \times 10^5, 7.326 \times 10^6, 2.803 \times 10^3)$ , the well index is prescribed for all three wells by  $WI = 50000$ , the bottom hole pressures are  $p_{V_1, bhp} = 265$ ,  $p_{V_2, bhp} = 105$  and  $p_{V_3, bhp} = 110$ . All the outer boundaries have Neumann type boundary condition. The numerical pressure belongs to the interval  $[105.121 : 264.872]$ , i.e. remains within the bounds provided by the pressure on the wells. The pressure and the Darcy velocity magnitude in a grid slice are presented in Fig. 4.

## Conclusion

We have introduced the first-order finite-volume method for the mixed formulation of the Darcy problem. The method does not suffer from the LBB-type instability although pressure and its gradient are collocated at cell centers. The future

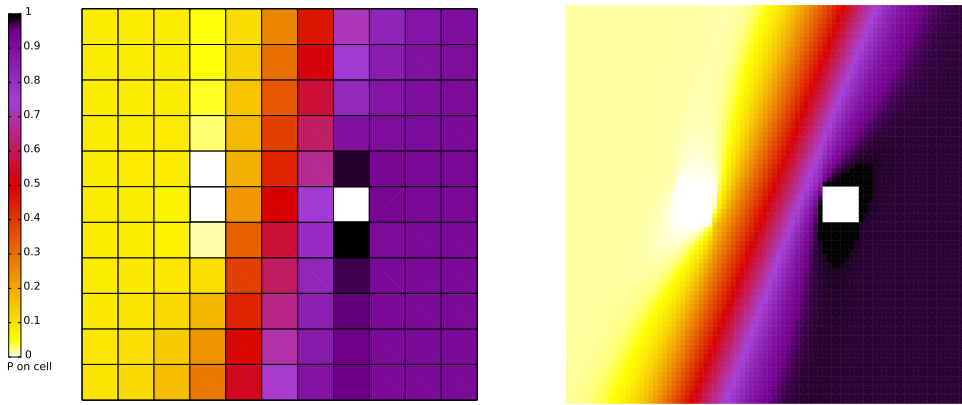


**Fig. 2.** Pressure in test with two wells on  $11 \times 11$  grid (left) and  $88 \times 88$  grid (right). (For interpretation of the colors in the figure(s), the reader is referred to the web version of this article.)

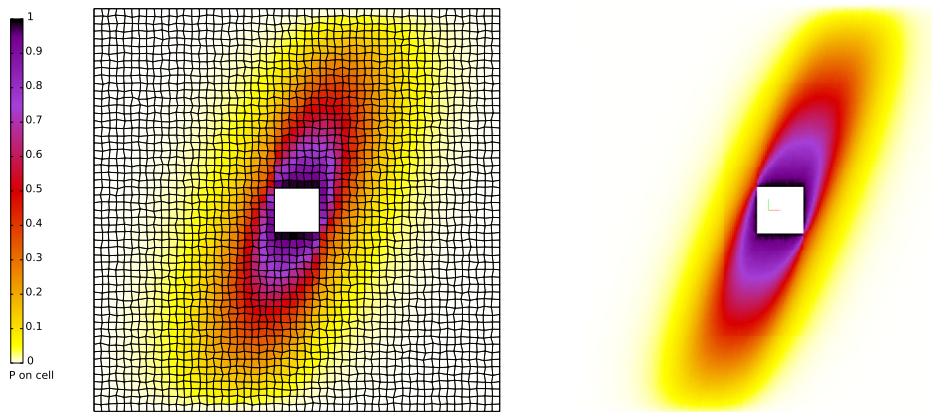


**Fig. 3.** Pressure in test with single well on  $54 \times 54$  grid (left) and  $216 \times 216$  grid (right).

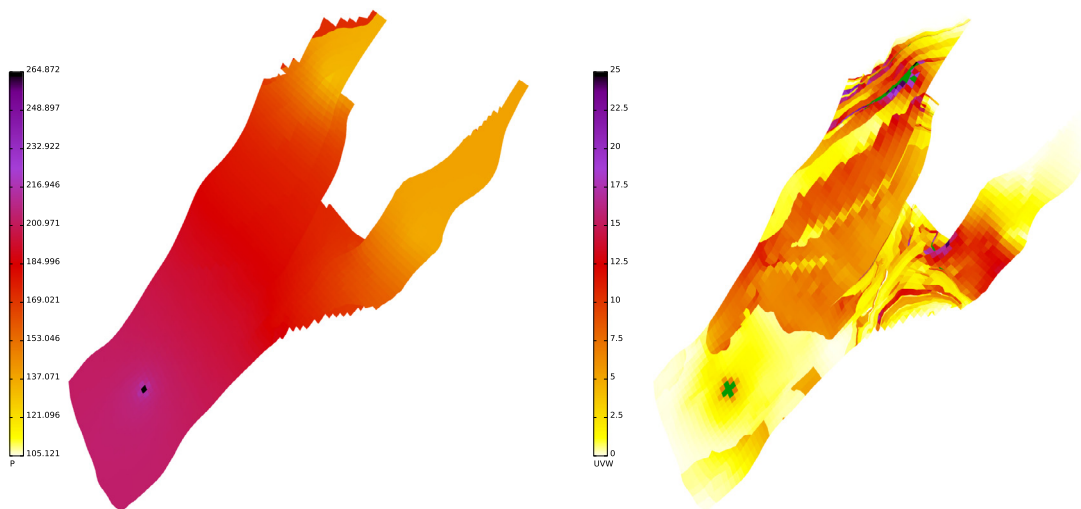


**Fig. 4.** Pressure (left) and Darcy velocity magnitude (right) in a grid slice of the Norne field grid. The green color on the image with velocity magnitude indicates that velocity is over 25.

directions are extension of the method to the second order of accuracy, applications to nonlinear multiphase flows, and other problems such as the Biot equations and the incompressible elasticity equations.

## Acknowledgement

This work was supported by the Russian Science Foundation through the grant 18-71-10111.

## References

- [1] O.A. Ladyzhenskaya, *The Mathematical Theory of Viscous Incompressible Flow*, vol. 12, Gordon & Breach, New York, 1969.
- [2] J. Droniou, Finite volume schemes for diffusion equations: introduction to and review of modern methods, *Math. Models Methods Appl. Sci.* 24 (08) (2014) 1575–1619.
- [3] V.I. Lebedev, Difference analogues of orthogonal decompositions, basic differential operators and some boundary problems of mathematical physics. I, *USSR Comput. Math. Math. Phys.* 4 (3) (1964) 69–92.
- [4] F.H. Harlow, J.E. Welch, Numerical calculation of time-dependent viscous incompressible flow of fluid with free surface, *Phys. Fluids* 8 (12) (1965) 2182–2189.
- [5] B. Perot, Conservation properties of unstructured staggered mesh schemes, *J. Comput. Phys.* 159 (1) (2000) 58–89.
- [6] C. Rhie, W.L. Chow, Numerical study of the turbulent flow past an airfoil with trailing edge separation, *AIAA J.* 21 (11) (1983) 1525–1532.
- [7] A. Settari, K. Aziz, et al., Use of irregular grid in reservoir simulation, *Soc. Pet. Eng. J.* 12 (02) (1972) 103–114.
- [8] P. Bonnet, X. Ferrieres, B. Michielsen, P. Klotz, J. Roumiguières, *Finite-Volume Time Domain Method*, Academic Press, San Diego, CA, 1999.
- [9] C. Oosterlee, H. Ritzdorf, Flux difference splitting for three-dimensional steady incompressible navier–stokes equations in curvilinear co-ordinates, *Int. J. Numer. Methods Fluids* 23 (4) (1996) 347–366.
- [10] E.F. Toro, *Riemann Solvers and Numerical Methods for Fluid Dynamics: a Practical Introduction*, Springer Science & Business Media, 2013.
- [11] R. Eymard, T. Gallouët, R. Herbin, Finite volume methods, *Handb. Numer. Anal.* 7 (2000) 713–1018.
- [12] G. Stoyan, On maximum principles for monotone matrices, *Linear Algebra Appl.* 78 (1986) 147–161.
- [13] L. Elsner, V. Mehrmann, Convergence of block iterative methods for linear systems arising in the numerical solution of euler equations, *Numer. Math.* 59 (1) (1991) 541–559.
- [14] M. Benzi, G.H. Golub, J. Liesen, Numerical solution of saddle point problems, *Acta Numer.* 14 (2005) 1–137.
- [15] A. George, K.D. Ikramov, On closedness of certain classes of matrices with respect to pseudoinversion, *Comput. Math. Math. Phys.* 42 (2002) 1242–1246.
- [16] R. Herbin, F. Hubert, Benchmark on discretization schemes for anisotropic diffusion problems on general grids, in: *Finite Volumes for Complex Applications V*, Wiley, 2008, pp. 659–692.
- [17] Z. Gao, J. Wu, A linearity-preserving cell-centered scheme for the heterogeneous and anisotropic diffusion equations on general meshes, *Int. J. Numer. Methods Fluids* 67 (12) (2011) 2157–2183.
- [18] M. Pal, M.G. Edwards, q-families of cvd (mpfa) schemes on general elements: numerical convergence and the maximum principle, *Arch. Comput. Methods Eng.* 17 (2) (2010) 137–189.
- [19] G. Manzini, M. Putti, Mesh locking effects in the finite volume solution of 2-d anisotropic diffusion equations, *J. Comput. Phys.* 220 (2) (2007) 751–771.
- [20] K.M. Terekhov, B.T. Mallison, H.A. Tchelepi, Cell-centered nonlinear finite-volume methods for the heterogeneous anisotropic diffusion problem, *J. Comput. Phys.* 330 (2017) 245–267.
- [21] D.S. Kershaw, Differencing of the diffusion equation in lagrangian hydrodynamic codes, *J. Comput. Phys.* 39 (2) (1981) 375–395.
- [22] B. Flemisch, K. Flornes, K. Lie, A. Rasmussen, Opm: the open porous media initiative, in: *AGU Fall Meeting Abstracts*, 2011.